International Journal of Biochemistry and Cell Biology 177 (2024) 106699

Contents lists available at ScienceDirect

International Journal of Biochemistry and Cell Biology

journal homepage: www.elsevier.com/locate/biocel

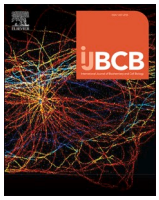

Use of Myriocin as co-adjuvant in glaucoma surgery: An *in vitro* study

Linda Montavoci [a,1], Dario Romano [b,1], Leonardo Colombo [b], Aida Zulueta [c], Michele Dei Cas [a], Mariangela Scavone [d], Delfina Tosi [e], Clara Bernardelli [f], Alessandro Autelitano [b], Marco Trinchera [g], Luca Rossetti [b,2], Anna Caretti [a,*,2]

[a] Department of Health Sciences, Biochemistry Laboratory, University of Milan, Via A. di Rudinì 8, Milan, Italy
[b] Eye Clinic, ASST Santi Paolo e Carlo Hospital, University of Milan, Via A. di Rudinì 8, Milan, Italy
[c] Istituti Clinici Scientifici Maugeri IRCCS, Neurorehabilitation Unit of Milan Institute, Via Camaldoli 64, Milan, Italy
[d] Department of Health Sciences, Haemostasis and Thrombosis Laboratory, University of Milan, Via A. di Rudinì 8, Milan, Italy
[e] Unit of Pathology, ASST Santi Paolo e Carlo Hospital, University of Milan, Via A. di Rudinì 8, Milan, Italy
[f] Department of Health Sciences, Pharmacology Laboratory, University of Milan, Via A. di Rudinì 8, Milan, Italy
[g] Dipartimento di Medicina e Chirurgia, University of Insubria, J.H. Dunant 5, Varese, Italy

ARTICLE INFO

Keywords:
glaucoma
myriocin
fibrosis
mitomycin C
myofibroblasts

ABSTRACT

Mitomycin C as well as other antiproliferative drugs are off-label agents widely used to prevent the failure of glaucoma surgery due to activation of Tenon's fibroblasts and the ensuing excessive subconjunctival scarring. Though efficacious, these treatments are associated with some severe long-term complications, so it is crucial to investigate less cytotoxic compounds as adjuvant therapy in glaucoma surgery. The aim of this study was to evaluate the effect and potential cytotoxicity of Myriocin, a natural sphingolipid synthesis inhibitor, on TGF-β1-induced myofibroblasts transformation of human dermal fibroblasts. We found that myriocin significantly attenuated the transcript levels of αSMA, CTGF, and MMP9 which are involved in the fibrosis process. Mitomycin C poorly affects the same pro-fibrotic markers while reducing fibroblasts motility as much as myriocin. At similar doses, five minutes of mitomycin C treatment consistently affects human dermal fibroblast viability and proliferation compared to prolonged myriocin application, strengthening already published data on the good tolerability of this natural compound. Our results draw attention to the use of myriocin as an adjuvant in glaucoma surgery due to the effectiveness in reducing fibroblasts to myofibroblasts transformation and the low cytotoxicity.

1. Introduction

Glaucoma is still the first cause of irreversible vision loss. In 2020 it was estimated a number of people with glaucoma worldwide of 80 million, with more than 11 million affected by bilateral blindness (Quigley, 1996). Surgical treatment is required when medical therapy fails to control intraocular pressure, or when functional and structural damage progresses despite apparently well-controlled pressure. The most common and effective surgical techniques aim to reduce intraocular pressure by creating a subconjunctival filtering bleb for aqueous outflow. The success of the surgery can be threatened by the excessive subconjunctival scarring, mainly due to the transformation of Tenon's

Abbreviations: TGF-β1, transforming growth factor β1; DMEM, Dulbecco's modified Eagles's medium; RPMI, Roswell Park Memorial Institute Medium; FBS, fetal bovine serum; EDTA, Ethylenediaminetetraacetic acid; THP1, Tohoku Hospital Pediatrics-1; PBS, phosphate buffer saline; GAPDH, Glyceraldehyde-3-phosphate dehydrogenase; RIPA, Radioimmunoprecipitation assay buffer; BCA, Bicinchoninic acid; DAPI, 4′,6-diamidino-2phenylindole; HEPES, 4–2-hydroxyethyl-1-piperazineethanesulfonic acid; αSMA, α Smooth Muscle Actin; CTGF, Connective Tissue Growth Factor; MMP9, Matrix metalloproteinase 9.

* Corresponding author.
E-mail addresses: linda.montavoci@unimi.it (L. Montavoci), dario.romano1@unimi.it (D. Romano), leonardo.colombo@unimi.it (L. Colombo), aida.zuluetamorales@icsmaugeri.it (A. Zulueta), michele.deicas@unimi.it (M.D. Cas), mariangela.scavone@unimi.it (M. Scavone), delfina.tosi@unimi.it (D. Tosi), clara.bernardelli@unimi.it (C. Bernardelli), alessandro.autelitano@unimi.it (A. Autelitano), marco.trinchera@uninsubria.it (M. Trinchera), luca.rossetti@unimi.it (L. Rossetti), anna.caretti@unimi.it (A. Caretti).

[1] These authors equally contributed
[2] These authors equally contributed

https://doi.org/10.1016/j.biocel.2024.106699
Received 30 August 2024; Received in revised form 18 November 2024; Accepted 19 November 2024
Available online 19 November 2024
1357-2725/© 2024 The Author(s). Published by Elsevier Ltd. This is an open access article under the CC BY-NC-ND license (http://creativecommons.org/licenses/by-nc-nd/4.0/).

fibroblasts into myofibroblasts which are responsible for increased synthesis of extracellular matrix proteins (Schlunck et al., 2016). Several studies have demonstrated that the suppression of fibroblast activation is crucial to prevent filtering bleb scarring. To avoid surgery failure, anti-proliferative substances such as 5-fluorouracil (5-FU) and mitomycin C (MMC) have been widely used in the last decades during and after the surgical procedure. Despite the progressive increase in the concentration and exposure time of these substances, the 5-year failure rate of glaucoma surgery is still between 39 % and 48 % (Gedde et al., 2022). Moreover, the use of these agents, which is often off-label, is associated with some complications, such as wound leakage, corneal toxicity, blebitis and endophthalmitis (Wilkins et al., 2005). These reasons have led in recent years to an increasing interest in evaluating different strategies to reduce surgical induced fibrosis, ranging from using anti-fibrotic molecules, targeting up- or down-regulated microRNAs and developing new drug delivery systems (Shao et al., 2023; Wolters et al., 2021; Yu et al., 2022). Some compounds, such as Paclitaxel, Lovastatin, Epigallocatechin-3-gallate, josamycin (Lin et al., 2020a; Stahnke et al., 2020) and Niclosamide (Zhang et al., 2023) have demonstrated good efficacy in *in vitro* studies by inhibiting the differentiation of human Tenon's fibroblast into myofibroblast, thus blocking the production of extracellular matrix proteins responsible of scarring (Lin et al., 2020a; Choritz et al., 2010; Meyer-ter-Vehn et al., 2008). Other molecules have also been tested *in vivo*: compounds like Doxycycline, Rosiglitazone and even engineered anti-fibrotic antibodies, have shown good efficacy in inhibiting fibroblast activation, the production of extracellular matrix proteins and the subconjunctival fibrosis in a rabbit model of glaucoma filtration surgery (Zhang et al., 2019; Sen et al., 2010; Shukla et al., 2023; Hassanpour et al., 2022). Few of these compounds have reached clinical trials, and none has been approved for the purpose of reducing glaucoma surgery-related fibrosis. Other approaches with demonstrated efficacy for various ocular conditions have also been tested to mitigate fibrosis in glaucoma patients. Treatments involving beta radiation exposure or anti-vascular endothelial growth factor injections have shown promising efficacy in surgical trials. However, their safety profiles were insufficient for clinical approval (Kirwan et al., 2012; Slabaugh and Salim, 2017).

The primary challenge in searching adjuvants for glaucoma surgery is to compare their effectiveness with MMC. In fact, despite its known limitations, MMC remains the gold standard due to its high efficacy.

Myriocin (Myr) is a natural compound derived from thermophilic fungi such as Mycelia Sterilia and Isaria Sinclarii, with a strong immunosuppressive activity (Miyake et al., 1995). Myr acts inhibiting the serine palmitoyltransferase enzyme (SPT), which regulates the first step in the sphingolipid synthesis. Myr has been studied in *in vitro* and in animal model of various diseases, like cystic fibrosis, ischemia-reperfusion injury and retinitis pigmentosa. It has demonstrated good efficacy in inhibiting inflammatory reaction and apoptosis, which are the pathophysiological bases of these conditions, without showing relevant side effects (Signorelli et al., 2021; Bonezzi et al., 2019; Platania et al., 2019a). Furthermore, the antifibrotic effect of Myr has been described in pulmonary (Gorshkova et al., 2012) and liver fibrosis (Jiang et al., 2019a).

In this study we used human dermal fibroblast (HDF) because human Tenon's fibroblasts (HTF) are not yet available. At the very beginning of our study, we obtained HTFs from patient biopsies but we experienced an excessive long-lasting cell expansion timing in order to gain the adequate cell number for the multiple analysis. Both HDFs and HTFs exhibited similar culture outgrowth and quite easy originated monolayers. However, HDFs are less influenced by the characteristics of the donor (Falco et al., 2013) and HTFs from surgical biopsies of Tenon's capsule samples are often contaminated by conjunctival cells (Park et al., 2016). The current experimental study was conducted to evaluate the efficacy and cytotoxicity of Myr compared to MMC in inhibiting the activation of human dermal fibroblasts in response to TGF-β1-stimulation and mechanically induced damage in order to explore its potential role as adjuvant in glaucoma surgery.The current experimental study was conducted to evaluate the efficacy and cytotoxicity of Myr compared to MMC in inhibiting the activation of human dermal fibroblasts in response to TGF-β1-stimulation and mechanically induced damage in order to explore its potential role as adjuvant in glaucoma surgery.

2. Material and methods

2.1. Reagents

The following materials were purchased: DMEM, RPMI and FBS from EuroClone Life Science Division (Milan, Italy); penicillin/streptomycin, Trypsin, Myriocin and Mitomycin C from Sigma-Aldrich (Burlington, MA, USA); protease inhibitors from Roche Italia (Monza, MB, Italy); SYBR Green system from Takara (Kusatsu, Japan); ReliaPrep™ Miniprep RNA extraction System and GoScript Reverse Transcription Mix from Promega (Madison, WI, USA); synthetic oligonucleotides from Eurofins Genomics (Ebersberg, Germany). TGF-β1 was purchased from Elabscience (Houston, TX, USA). Methanol, acetonitrile and other reagents for sphingolipid (SPL) mass spectrometry analysis (all analytical grade) were supplied from Merck (Darmstadt, Germany). Water was MilliQ grade. All reagents were of the maximal available purity degree.

2.2. Stock solutions

Commercially available TGF-β1 solution (0.2 mg/mL; #PKSH032007, Elabscience) was pre-diluted 1:1000 with water to obtain the stock solution concentration of 200 ng/mL.

Myriocin powder (#M1177, Sigma-Aldrich) was dissolved in dimethyl sulfoxide (DMSO) by warming up to 37 °C to obtain the stock solution concentration of 5 mM. Aliquots of the stock solution were stored at −20°C until use.

Mitomycin C was commercially available as stock solution (10 mg/mL; #M5353, Sigma).

2.3. Cell culture

Human dermal fibroblasts (HDF) were from Innoprot (#P10858, Bizkaia, Spain) and were used instead of human Tenon's fibroblasts (HTF) which are not yet available. HDF were grown in T25 culture flasks in DMEM supplemented with 10 % FBS and 1 % penicillin/streptomycin antibiotic solution. At about 90 % of confluence, corresponding to 1.2–1.3 $\times 10^6$, they were detached by trypsin/EDTA and seeded in dishes or multiwell plates of various sizes as detailed in the following experimental sections. THP1, a human monocyte cell line from ATCC TIB-202 kindly provided by Dr Massimo Locati (University of Milan and Humanitas Research Hospital) was used for viability assay. They were maintained in RPMI-1640 supplemented with 10 % FBS and 1 % penicillin/streptomycin until they reach about 1.0–1.5 $\times 10^6$ cells/mL density.

2.4. Cell treatment

Twenty-four hours upon seeding, fibroblasts were organized in six different groups and treated as follows:

- Control: no pre-treatment nor treatment at all
- TGF-β1: no pretreatment, TGF-β1 only 24 h (Wu et al., 2020)
- TGF-β1+Myr: pre-treatment Myr, 50 μM for 1 hour, no wash then TGF-β1 24 h
- TGF-β1+MMC: pre-treatment MMC, 20 μg/mL for 5 minutes, wash-out with PBS then TGF-β1 24 h
- Myr: pre-treatment Myr, 50 μM for 1 hour, no wash
- MMC: pre-treatment MMC, 20 μg/mL for 5 minutes, wash-out with PBS (Wilkins et al., 2005)

Twenty μg/mL of MMC correspond to 60 μM, similar to the Myr concentration. Moreover, this was also the higher concentration suggested by the manufacturer. Viability and proliferation assays were carried out at 24; 48; 72 and 96 hours after the end of pre-treatments, the scratch wound assay at 24 and 48 hours. For viability assay, THP1 were organized in three experimental groups of treatment as detailed for HDF and analyzed at 96 hours. Cell treatments and related assays are detailed in Supplementary Figure 1.

2.5. Sphingolipid' determination by LC-MS/MS

For the sphingolipid' analysis, HDF were plated in 60 mm tissue culture dishes (2.5×10^5 cells/dish) for 48 hours before the established treatment with TGF-β1 w/out Myr. After 24 hours of treatment, cells were detached, centrifuged for 6 minutes at 100 xg, the pellets washed twice in PBS 1X, spun again for 5 minutes at 500 xg at 4°C and finally resuspended in 100 μL of PBS 1X with protease inhibitors cocktail. Ceramide (Cer) and dihydroceramide (DHCer) analysis was performed as previously described (Zulueta et al., 2019). Briefly, Cer and DHCer were extracted with a cold methanol/chloroform mixture (850 μL, 2:1, v/v) coupled with alkaline methanolysis (75 μL KOH 1 M, 2 h at 38 °C) and the lipid content normalized to the total protein amount (mg). The LC-MS/MS consisted of an LC Dionex 3000 UltiMate (Thermo Fisher Scientific) coupled to a tandem mass spectrometer AB Sciex 3200 QTRAP (AB Sciex, Concord, ON, Canada) equipped with electrospray ionization TurboIonSpray™ source operating in positive mode (ESI+).

2.6. RNA extraction and RT-qPCR

2.5×10^5 HDF were plated in 60 mm tissue culture dishes for 48 hours before the established treatment protocol lasting 24 hours. qPCR was performed using cDNA from the four different groups of treatment. The RNA extraction and reverse transcription were performed as previously described (Zulueta et al., 2019). Human gene primer sequences for aSMA, CTGF, MMP-9, GAPDH are reported in Supplementary Material (Supplementary Figure 2). RT-qPCR was executed on StepOnePlus Real-Time PCR Systems (Thermofisher). Results were normalized on GAPDH and the 2-ΔΔCt method was used to calculate the relative value of gene expression vs control cells (Arocho et al., 2006).

2.7. Protein extraction and Western Blotting

4.0×10^5 HDF were plated in 100 mm tissue culture dishes for 48 hours before the established treatment protocol lasting 24 hours. Cell proteins were extracted using Radioimmunoprecipitation assay (RIPA) buffer and their concentration determined by Pierce™ BCA Protein Assay Kit. Twenty μg of protein from each sample were separated on 10 % SDS-PAGE gel and transferred onto a nitrocellulose membrane via electroblotting. Following TBS-T (Tris-HCl buffer saline with Tween) washes and incubation with 5 % nonfat dry milk for 1 hour at room temperature, the membrane was incubated overnight at 4 °C with anti-αSMA primary antibody (1:10000, Abcam, ab124964 [EPR5368]). Anti-tubulin antibody (1:1000, Santa Cruz, #12462-R) was used as loading control. The membrane was further blotted with horseradish peroxidase-conjugated secondary antibody (1:10000, anti-IgG, Jackson). The protein bands were detected by chemo-luminescent method by the Alliance™ UVITEC (Cambridge, UK) system which provided the band intensity quantification as well.

2.8. Immunofluorescence

1.0×10^4 HDF (corresponding to 25 % of confluence) were plated in 48 well plates. After 48 hours, HDF underwent the established treatment protocol lasting 24 hours. The cells were washed twice with PBS 1X and fixed with 3.7 % formaldehyde for 10 minutes. After two additional washes with PBS containing 1 % bovine serum albumin (BSA) and 0.05 % TritonX100 to facilitate membrane permeabilization, the cells were exposed to anti-Collagen I antibody (Abcam, ab138492 [EPR7785]) diluted 1:100 in 1 % BSA - 0.05 % TritonX100 - PBS for 1 hour at room temperature. After fixation, cells were then subjected to two washes as previously described, followed by incubation in the dark (1 hour at room temperature) with Alexa Fluor™488 secondary antibody (1:1000, # A32731, Invitrogen). The cells were additionally incubated with 300 nM DAPI for 5 minutes at room temperature in the dark and finally examined by fluorescence microscopy.

2.9. Scratch wound assay

HDFs were seeded into each chamber of a Culture-Insert 3 Well, that ensures a 500 μm (+/- 100 μm) width of cell-free gap (Ibidi, Gräfelfing, Germany). This chamber allows to standardize the assay since cells migrate in a defined area and to prevent the surface damaging due to the manual scratch. The inserts were placed in a 24-multiwell plate and 10^4 fibroblasts, resuspended in 150 μL of cell culture medium, were grown until they reach the confluence. After insert removal, the wells were washed twice with PBS and fibroblasts supplemented with fresh culture medium and subjected to the established treatment with Myr or MMC. The images were taken with the Axio Vert.A1 FL microscope (Zeiss, Germany) 24 and 48 hours after the end of the treatment. For each picture, the percentage of open area was calculated using the ImageJ/Fiji® plugin Wound healing size tool (Suarez-Arnedo et al., 2020).

2.10. Phosphatidilserine expression using fluorescein-labelled Annexin V

HDF (3.0×10^4 cells/well) and THP-1 (2.0×10^5 cells/well) were plated in 48-wells for 48 hours prior to treatment with Myr and MMC and analyzed 24 and 96 hours later. HDF were detached with accutase for 10 minutes at 37°C. Both cell lines were then centrifuged for 6 minutes at 100 xg and washed twice with cold PBS 1X. HDF pellets were resuspended in 50 μL of binding buffer 1X (HEPES 10 mM, NaCl 140 mM, $CaCl_2$ 2.5 mM). THP-1 pellets were resuspended in the same buffer to achieve a concentration of 1.0×10^5 cells/mL. Fifty microliters of the cells' suspensions were stained with allophycocyanin (APC)-conjugated AnnexinV (BD Biosciences, #550475) for 15 minutes in the dark and finally diluted 1:6 with PBS 1X for flow cytometry analysis. HDF and THP-1 were gated for side and forward scatter and a total of 2000 events were acquired at low flow rate using the FACS Verse Cytometer (BD Biosciences, San Jose, CA). Data were analyzed using FACS Suite software (BD Biosciences) and results were expressed as percentage of Annexin V positive cells.

2.11. CFSE proliferation assay

HDF were plated in 48-wells (25 % confluency, corresponding to 1.0×10^4 cells/well). After two days, 10 μM carboxyfluorescein succinimidyl ester (CFSE, BD Biosciences, # 5244927) was added to each well and the cells were treated as previously described with Myr or MMC. The CFSE dye signal (emission 488 nm) was analyzed at different time points (24, 48, 72 and 96 hours) by flow cytometry using FACS Verse Cytometer (BD Biosciences, San Jose, CA). The median intensity of each sample was reprocessed as stated below, to express it as the percentage of proliferation relative to the control:

[(FITC Median Intensity Time point 0 / FITC Median Intensity Time point X) - 1] x 100

The data are represented as fold change over control.

2.12. Statistical analysis

Data significance was assessed by Kruskal-Wallis test ($p<0.05$) followed by the Benjamini–Hochberg multiple comparison test when significant ($p<0.05$). All data are expressed as mean ± SEM.

3. Results

3.1. Sphingolipids' determination by LC-MS/MS

Myr reduces the expression of ceramide (Cer) and its precursor dihydro-ceramide (DHCer) by inhibiting serine palmitoyltransferase (SPT), the enzyme that regulates the rate limiting step of sphingolipid synthesis. We therefore preliminarily investigated Myr effects on Cer accumulation in fibroblasts stimulated with 5 ng/mL TGF-β1. As shown in Fig. 1, 24 hours of co-treatment with 50 μM Myr lowered TGF-β1-induced accumulation of Cer (1B) and DHCer (1 A), suggesting the interplay between TGF-β1 and sphingolipid biosynthetic pathway.

3.2. Myriocin treatment reduces fibrosis markers and collagen deposition

Several markers of the fibrotic process were evaluated. We focused on αSMA, which is expressed when fibroblasts transform into mature, active myofibroblasts, CTGF, a peptide produced by fibroblasts with pro-fibrotic properties, and MMP9 which is produced by fibroblasts to facilitate the degradation of the extracellular matrix, thereby promoting their infiltration. The transcript levels of all the markers were lowered after the treatment with Myr (Fig. 2A, B, C) as well as the protein expression of αSMA, sharing a similar trend (Figs. 2D and 2E). Except for αSMA, the other fibrotic markers' transcripts were not affected by MMC (Figs. 2A, 2B, 2C).

TGF-β1 treatment led to an increase of collagen expression compared to control HDF (Fig. 3A), as evidenced by the raising of the green staining (Fig. 3B) by immunofluorescence analysis. The co-administration of Myr almost restored the control amount of collagen (Fig. 3C) that was unchanged upon MMC co-treatment (Fig. 3D). The collagen stain was quantified as: (DAPI and collagen positive cells)/(total DAPI positive cells)*mean intensity of collagen fluorescence. Results are reported as bar histograms (Fig. 3E).

3.3. Myriocin attenuates fibroblasts motility

To evaluate cell motility, the scratch wound assay was performed and the cells observed for 24 and 48 hours. The scratch wound was almost fully repaired at 48 hours in control fibroblasts (Fig. 4A, left panels). Pre-treatment with Myr (Fig. 4A, middle panels) or MMC (Fig. 4A, right panels) attenuated cell migration and no significant difference was observed between treatments (Fig. 4B).

3.4. Myriocin poorly affects viability and proliferation of fibroblasts

To evaluate the cytotoxicity of Myr versus MMC, HDF viability was analyzed by Annexin, an early apoptosis marker, 24 h after the end of the pre-treatment. We also investigated a long-lasting time point (96 hours) to mimic MMC reported long-term complications (Wilkins et al., 2005). Twenty-four hours after MMC treatment, HDFs exhibited significantly higher Annexin levels compared to the control, whereas a moderate, though not significant increase, was observed following Myr supplementation (Fig. 5A). As expected, MMC showed long lasting antimitotic effects beyond the cell phenotype. In fact, at 96 hours Annexin-positive cells almost doubled in the MMC compared to the untreated group in both HDFs (Fig. 5B) and THP-1 (Fig. 5C), a human monocyte cell line likely involved in tissue inflammation characteristic for fibrogenesis. Furthermore, the CFSE assay demonstrated that, from 48 h on, MMC slows down the proliferation of HDF which is likely unaffected by Myr, as depicted in Fig. 5D.

4. Discussion

In this study we investigated the anti-fibrotic potential of Myr on TGF-β1-induced myofibroblast transformation of human dermal fibroblasts and on wound-healing process. We observed that Myr is more efficacious and less cytotoxic compared to MMC. The main issue for the failure of glaucoma filtration surgery is the sub-conjunctival fibrosis, which results from the transformation of fibroblasts into myofibroblasts in response to injury or inflammation (Roberts et al., 2003; Saika et al., 2008). While reducing the risk of scar formation, anti-proliferative substances such as MMC are associated with short- and long-term complications (Wilkins et al., 2005). Thus, there is an unmet need to identify novel, less cytotoxic anti-fibrotic compounds as co-adjuvants in glaucoma surgery. Epigallocatechin-3-gallate has shown effectiveness comparable to MMC in *in vitro* studies but is known to induce mitochondrial membrane collapse and ROS formation at higher doses (Lin et al., 2020a). Niclosamide and Josamycin have demonstrated strong inhibitory effects on the activation, proliferation, and migration of fibroblasts exposed to TGF-β1 (Stahnke et al., 2020; Zhang et al., 2023),

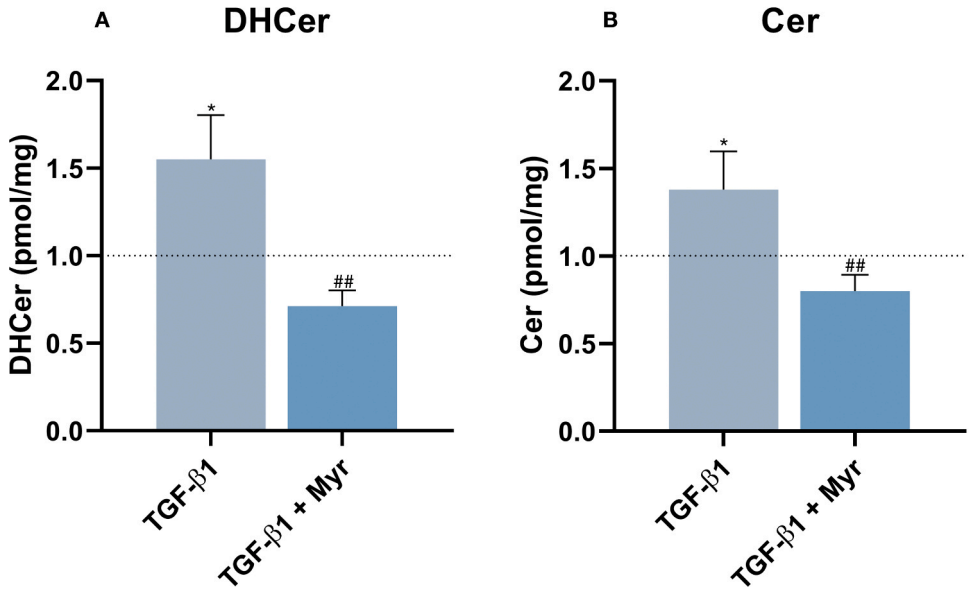

Fig. 1. DHCer and Cer content. DHCer (**A**) and Cer (**B**) levels are quantified in TGF-β1- and TGF-β1+Myr-treated groups from six independent experiments. All the values are expressed as the mean±SEM and presented as fold change over the control (dotted line). *=p<0.05 vs control (dotted line); #=p<0.05 vs TGF-β1.

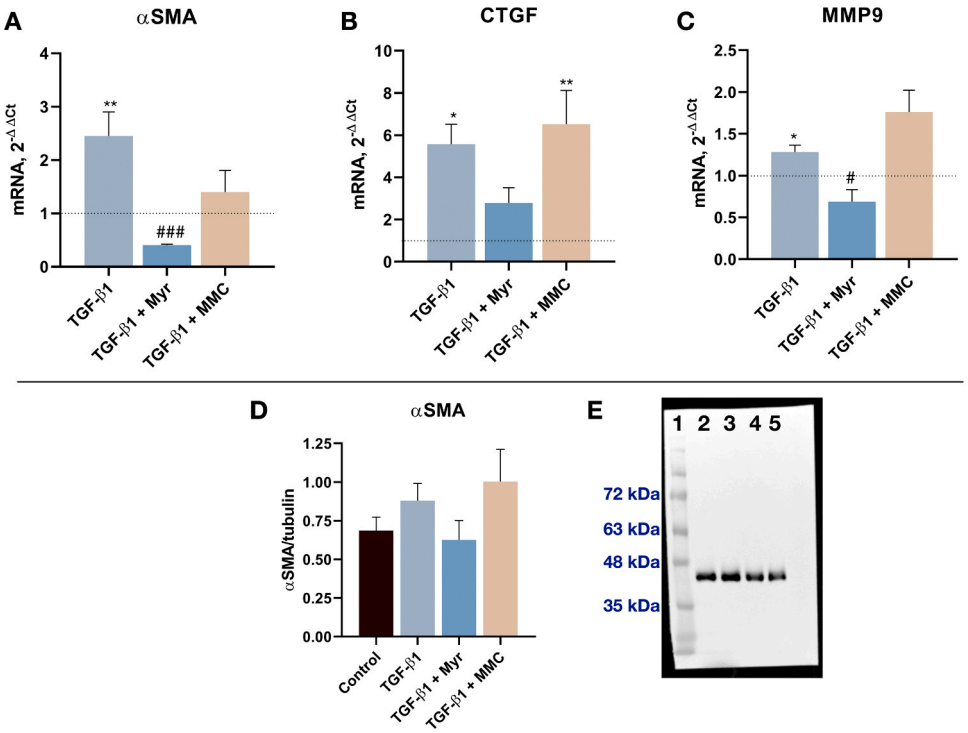

Fig. 2. Fibrosis markers' expression. Transcript levels of αSMA (**A**), CTGF (**B**) and MMP9 (**C**) are expressed as fold change over the control (dotted line) in TGF-β1-, TGF-β1+Myr- and TGF-β1+MMC-treated groups (five independent experiments). Bars histogram (**D**) reports αSMA protein expression quantification from seven independent experiments. All data were normalized on tubulin expression as loading control (Supplementary figure 3). The Western blotting image (**E**) is the most representative. Lane 1: molecular weight markers; lane 2: control group; lane 3: TGF-β1-treated group; lane 4: TGF-β1+Myr-treated group; lane 5: TGF-β1+MMC-treated group. All the values are expressed as the mean±SEM. *=p<0.05 and **=p<0.01 vs control (dotted line); #=p<0.05 and ###= p<0.001 vs TGF-β1.

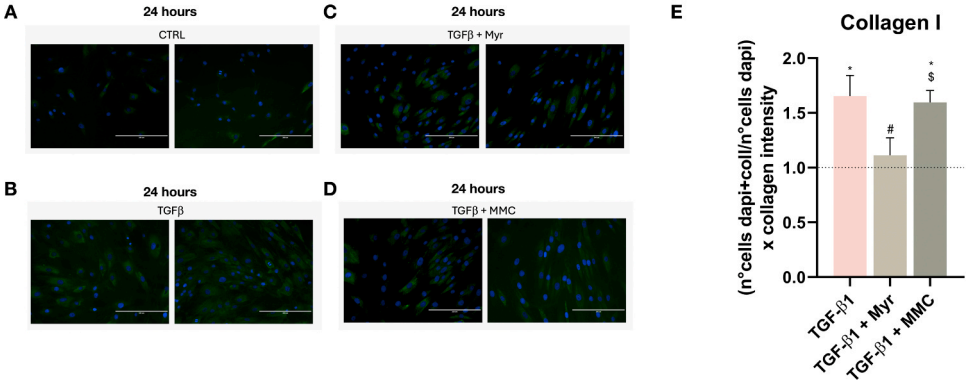

Fig. 3. Collagen deposition. The immunofluorescence images report collagen staining in green and nuclei staining in blue (DAPI). Panels **A, B, C, D** report two representative images out of six independent experiments. Bar histograms (**E**) show the quantification of collagen-positive cells from six independent experiments and are expressed as fold change over the control (dotted line). All the values are expressed as the mean±SEM. *=p<0.05 vs control (dotted line); #=p<0.05 vs TGF-β1; $=p<0.05 vs TGF-β1+Myr-treated group.

primarily mediated by the reduction of α-SMA expression. However, data on direct comparisons with MMC, as well as information on the local tolerability and safety are still lacking. We used human dermal fibroblast (HDF) because human Tenon's fibroblasts (HTF) are not yet available. When compared to HTFs, HDFs exhibited similar culture outgrowth after biopsy and demonstrated comparable behavior when exposed to collagenase and when incubated in autologous or fetal bovine serum. Homogenous monolayers of fibroblasts can be easily obtained from both Tenon and skin, with this second source less influenced by the age and the medical/surgical history of the donor (Falco et al., 2013). Moreover, surgical biopsies of Tenon's capsule samples are often contaminated by conjunctival cells and this contamination might complicate the analysis and the interpretation of the results (Park et al., 2016). Cellular injury and the ensuing acute inflammatory response promote TGF-β1 release that, in turn, stimulates recruitment, proliferation and metabolic activity of fibroblasts (Wynn, 2008; Barrientos et al., 2008). Fibroblasts' activation drives enhanced deposition of extracellular matrix (ECM) proteins and stabilization of the fibrotic scar tissue (Kendall and Feghali-Bostwick, 2014). The direct or indirect inhibition of the TGF-β1 pathway's activation is the strategy to counteract conjunctival fibrosis (Futakuchi et al., 2018; Yamanaka et al., 2006). The antifibrotic effect of Myr has been already described in two pathological conditions other than glaucoma. In a rat model of non-alcoholic fatty liver disease (NAFLD), chronic administration of Myr reduces

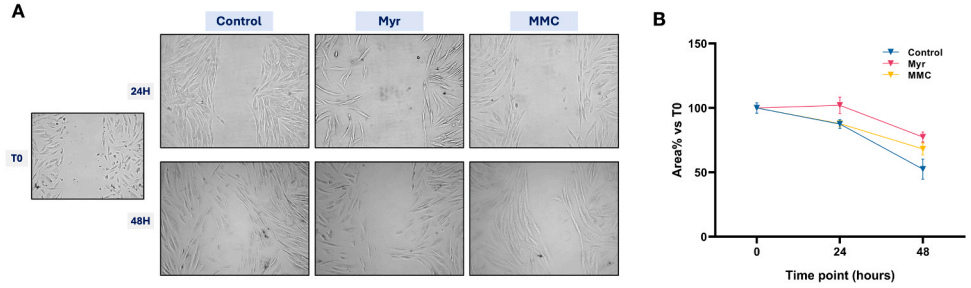

Fig. 4. Fibroblasts' motility. Panel **A.** The wound healing ability is evaluated in control untreated (Control), Myr-treated (Myr) and MMC-treated group (MMC) at two different timepoints (24 h and 48 h). Control T0 panel represents the wound width shortly after the insert removal. The most representative images out of four experiments are shown. Panel **B**. Percentage of wound open area versus T0 calculated using the ImageJ/Fiji® plugin Wound healing size tool.

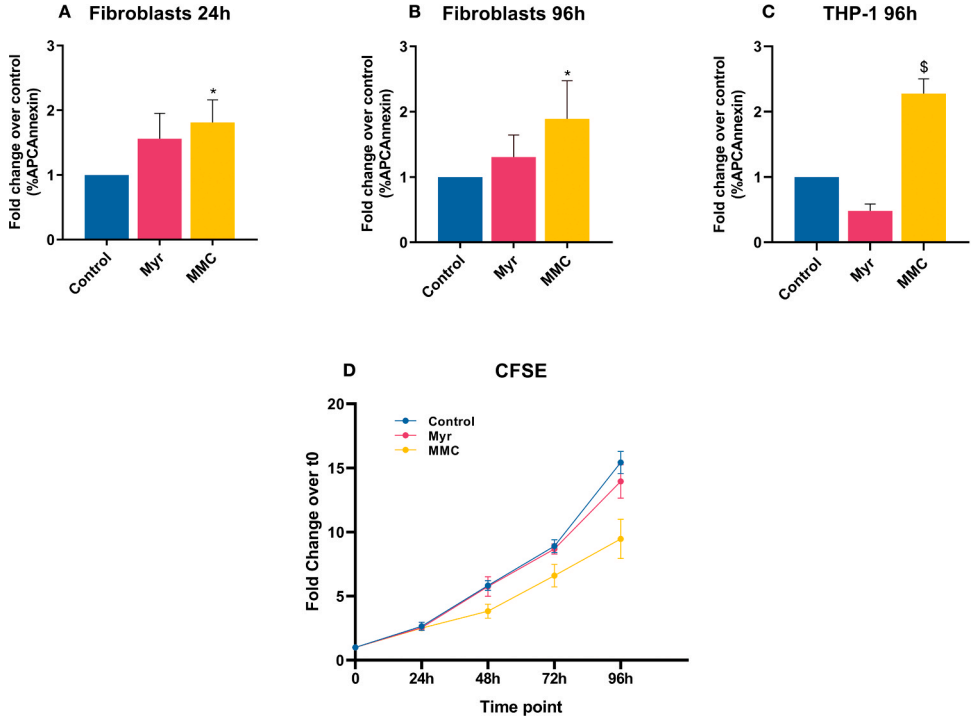

Fig. 5. Fibroblasts' viability and proliferation. Fibroblasts and THP-1 viability were assessed at 24h-96h (Fig. A and B) and 96 h (Figure C), respectively, by evaluating the Annexin-positive staining upon Myr and MMC pre-treatment. Results are expressed as fold change of Annexin-positive cells over the control untreated cells (% Annexin positive cells) from four different experiments. All data are presented as the mean±SEM. *=$p<0.05$ vs control and $^{\$}$=$p<0.05$ vs Myr. Fibroblasts' proliferation rate was analyzed by CFSE assay (Fig. 5D). Results are expressed as fold change over the control from four different experiments. All data are presented as the mean±SEM.

fibrosis in liver tissue samples together with apoptosis and inflammation (Jiang et al., 2019b). In a mouse model of radiation-induced pulmonary fibrosis, Myr-induced inhibition of SPT delays the onset of lung fibrosis and increases animal lifespan (Gorshkova et al., 2012) through the inhibition of bioactive sphingolipids. The same study reports that long-term treatment with Myr or silencing of SPT reduces αSMA upregulation in TGF-β1-stimulated normal human lung fibroblasts, suggesting SPT as a novel therapeutic target to manage lung fibrosis progression. The gain of Cer and DHCer content that we observed in TGF-β1-stimulated HDF and the decrease upon Myr treatment, sustain the interplay between TGF-β1 and sphingolipid pathways. Accordingly, in TGF-β1-activated HDF we showed that Myr significantly attenuates αSMA, CTGF, and MMP9 transcript levels which promote fibrosis controlling fibroblast activation and growth as well as extracellular matrix remodeling. Instead, the same pro-fibrotic markers were poorly affected by MMC that in turn attenuated fibroblasts motility as much as Myr. MMC is a chemotherapeutic antibiotic derived from Streptomyces caespitosus, inhibiting DNA synthesis. It is well known that MMC use in trabeculectomy wound healing relies on its anti-proliferative and pro-apoptotic effects on Tenon's capsule fibroblasts (Crowston et al., 1998). However, it has been recently reported that low dose MMC (0.02 μM or 0.2 μM) induces cellular senescence in trabeculectomy *in vitro* models and restrains α-SMA and collagen (COL1A1) transcripts in TGF-β1-stressed senescent HTFs (Lin et al., 2020b). In this study, we treated HDF with high dose MMC (60 μM corresponding to 20 μg/mL, the higher dose suggested by the manufacturer) highly exceeding the low-dose range that promotes fibroblasts senescence phenotype and the consequent decrease of pro-fibrotic markers thus probably accounting for MMC cytotoxic effects that we observed. Single shot, topic clinical application of MMC in humans lasts few minutes (Wilkins et al., 2005). In our model, 5 min treatment of HDF significantly elevates early markers of apoptosis at 24 and 96 hours upon treatment. Moreover, MMC exerts long lasting antimitotic effects beyond the cell phenotype, affecting the viability of THP-1 cells likely involved in inflammation peculiar to fibrogenesis. In addition, MMC slowed down the proliferation of HDF. Conversely, none of the above effects were detected upon

Myr treatment lasting 24 h. Indeed, we observed that prolonged administration (24 h) of Myr at similar concentration (50 μM), already experienced by our group in a different in vitro model (Signorelli et al., 2021) poorly affects cells viability and proliferation, highlighting the good tolerability of this natural compound. Accordingly, in animal models of Retinitis Pigmentosa, an inherited retinal dystrophy leading to irreversible visual impairment, Myr has been proved efficacious in preventing rods and cones degeneration and apoptosis. Single intravitreal or repeated topical transcorneal administration of eye drops containing Myr, did not induce adverse effects at general and ocular level (Piano et al., 2020, 2013; Platania et al., 2019b; Strettoi et al., 2010). There is evidence that prolonged systemic administration of Myr in different pathological settings is well tolerated by animal models, except for inadequate doses. After four weeks of intraperitoneal Myr treatment, mice subjected to diet-induced insulin resistance showed a complete reversal of glucose intolerance and improved oxygen consumption rates without weight loss (Ussher et al., 2010). Sixty days of intraperitoneal Myr injection in ApoE-deficient mice counteracted atherosclerotic development without affecting T cell populations (Hojjati et al., 2005)

In conclusion, these results draw attention to Myr as a potential adjuvant in glaucoma-associated surgery to reduce the excessive sub conjunctival scarring due to the transformation of Tenon's fibroblasts into myofibroblasts. Further experiments on Tenon's fibroblasts and preclinical animal models of glaucoma filtration surgery are needed in order to validate the anti-fibrotic effects of Myr.

Funding

This work was supported by the funds of the Eye Clinic of ASST Santi Paolo e Carlo Hospital.

CRediT authorship contribution statement

Clara Bernardelli: Writing – review & editing, Methodology. **Alessandro Autelitano:** Writing – review & editing. **Marco Trinchera:** Writing – review & editing, Methodology. **Dario Romano:** Writing – review & editing, Writing – original draft, Methodology, Formal analysis, Data curation, Conceptualization. **Leonardo Colombo:** Writing – review & editing, Writing – original draft. **Luca Rossetti:** Writing – review & editing, Funding acquisition, Formal analysis, Data curation, Conceptualization. **Anna Caretti:** Writing – review & editing, Supervision, Funding acquisition, Formal analysis, Data curation, Conceptualization. **Linda Montavoci:** Writing – review & editing, Writing – original draft, Methodology, Formal analysis, Data curation, Conceptualization. **Mariangela Scavone:** Writing – review & editing, Methodology. **Delfina Tosi:** Methodology. **Aida Zulueta:** Writing – review & editing, Validation, Formal analysis, Data curation. **Michele Dei Cas:** Methodology, Data curation.

Declaration of Competing Interest

The authors declare the following financial interests/personal relationships which may be considered as potential competing interests: Anna Caretti, Luca Rossetti, Leonardo Colombo and Dario Romano have patent pending to assignee. The other authors declare that they have no known competing financial interests or personal relationships that could have appeared to influence the work reported in this paper.

Acknowledgements

the authors thank Prof. Riccardo Ghidoni for his relevant suggestions in the conception of the study and Dr. Claudia Pasini for her technical support.

Appendix A. Supporting information

Supplementary data associated with this article can be found in the online version at doi:10.1016/j.biocel.2024.106699.

Data Availability

Data will be made available on request.

References

Arocho, A., Chen, B., Ladanyi, M., Pan, Q., 2006. Validation of the 2-DeltaDeltaCt calculation as an alternate method of data analysis for quantitative PCR of BCR-ABL P210 transcripts (Mar). Diagn. Mol. Pathol. 15 (1), 56–61. https://doi.org/10.1097/00019606-200603000-00009.

Barrientos, S., Stojadinovic, O., Golinko, M.S., Brem, H., Tomic-Canic, M., 2008. Growth factors and cytokines in wound healing (Sep). Wound Repair Regen. 16 (5), 585–601. https://doi.org/10.1111/J.1524-475X.2008.00410.X.

Bonezzi, F., et al., 2019. Sphingolipid synthesis inhibition by myriocin administration enhances lipid consumption and ameliorates lipid response to myocardial ischemia reperfusion injury (Aug). Front Physiol. 10 (JUL), 462263. https://doi.org/10.3389/FPHYS.2019.00986/BIBTEX.

Choritz, L., Grub, J., Wegner, M., Pfeiffer, N., Thieme, H., 2010. Paclitaxel inhibits growth, migration and collagen production of human Tenon's fibroblasts-potential use in drug-eluting glaucoma drainage devices (Nov). Graefe's Arch. Clin. Exp. Ophthalmol. 248 (2), 197–206. https://doi.org/10.1007/S00417-009-1221-4/FIGURES/7.

Crowston, J., Akbar, A., Constable, P., Occleston, N., Daniels, J., Khaw, P., 1998. Antimetabolite-induced apoptosis in Tenon's capsule fibroblasts (Feb). Invest Ophthalmol. Vis. Sci. 39 (2), 449–454 (Feb).

Falco, E.De, et al., 2013. A standardized laboratory and surgical method for in vitro culture isolation and expansion of primary human Tenon's fibroblasts (Jun). Cell Tissue Bank 14 (2), 277–287. https://doi.org/10.1007/S10561-012-9325-1/TABLES/5.

Futakuchi, A., et al., 2018. YAP/TAZ are essential for TGF-β2-mediated conjunctival fibrosis (Jun). Invest Ophthalmol. Vis. Sci. 59 (7), 3069–3078. https://doi.org/10.1167/IOVS.18-24258.

Gedde, S.J., et al., 2022. Treatment outcomes in the primary tube versus trabeculectomy study after 5 years of follow-up (Dec.). Ophthalmology 129 (12), 1344–1356. https://doi.org/10.1016/J.OPHTHA.2022.07.003.

Gorshkova, I., et al., 2012. Inhibition of serine palmitoyltransferase delays the onset of radiation-induced pulmonary fibrosis through the negative regulation of sphingosine kinase-1 expression[S]. J. Lipid Res. 53, 1553–1568. https://doi.org/10.1194/jlr.M026039.

Hassanpour, K., et al., 2022. The inhibitory effect of connective tissue growth factor antibody on postoperative fibrosis in a rabbit model of trabeculectomy (Oct). J. Ophthalmic Vis. Res 17 (4), 486–496. https://doi.org/10.18502/JOVR.V17I4.12300.

Hojjati, M.R., et al., 2005. Effect of myriocin on plasma sphingolipid metabolism and atherosclerosis in apoE-deficient mice (Mar). J. Biol. Chem. 280 (11), 10284–10289. https://doi.org/10.1074/JBC.M412348200.

Jiang, M., Li, C., Liu, Q., Wang, A., Lei, M., 2019a. Inhibiting ceramide synthesis attenuates hepatic steatosis and fibrosis in rats with non-alcoholic fatty liver disease (Sep). Front Endocrinol. (Lausanne) 10 (SEP), 480549. https://doi.org/10.3389/FENDO.2019.00665/BIBTEX.

Jiang, M., Li, C., Liu, Q., Wang, A., Lei, M., 2019b. Inhibiting ceramide synthesis attenuates hepatic steatosis and fibrosis in rats with non-alcoholic fatty liver disease (Sep). Front Endocrinol. (Lausanne) 10 (SEP). https://doi.org/10.3389/FENDO.2019.00665.

Kendall, R.T., Feghali-Bostwick, C.A., 2014. Fibroblasts in fibrosis: novel roles and mediators. Front Pharm. 5. https://doi.org/10.3389/FPHAR.2014.00123.

Kirwan, J.F., Rennie, C., Evans, J.R., 2012. Beta radiation for glaucoma surgery (Jun). Cochrane Database Syst. Rev. (6). https://doi.org/10.1002/14651858.CD003433.PUB3/MEDIA/CDSR/CD003433/IMAGE_N/NCD003433-CMP-003-03.PNG.

Lin, H.L., et al., 2020a. Epigallocatechin-3-gallate (EGCG) inhibits myofibroblast transformation of human Tenon's fibroblasts (Aug). Exp. Eye Res. 197. https://doi.org/10.1016/J.EXER.2020.108119.

Lin, L.T., et al., 2020b. Antifibrotic role of low-dose mitomycin-c-induced cellular senescence in trabeculectomy models (Jun). PLoS One 15 (6), e0234706. https://doi.org/10.1371/JOURNAL.PONE.0234706.

Meyer-ter-Vehn, T., Katzenberger, B., Han, H., Grehn, F., Schlunck, G., 2008. Lovastatin Inhibits TGF-β–induced myofibroblast transdifferentiation in human tenon fibroblasts (Sep). Invest Ophthalmol. Vis. Sci. 49 (9), 3955–3960. https://doi.org/10.1167/IOVS.07-1610.

Miyake, Y., Kozutsumi, Y., Nakamura, S., Fujita, T., Kawasaki, T., 1995. Serine palmitoyltransferase is the primary target of a sphingosine-like immunosuppressant, ISP-1/myriocin. Biochem Biophys. Res Commun. 211 (2), 396–403. https://doi.org/10.1006/BBRC.1995.1827.

Park, C.Y., Marando, C.M., Liao, J.A., Lee, J.K., Kwon, J., Chuck, R.S., 2016. Details of the collagen and elastin architecture in the human limbal conjunctiva, tenon's capsule and sclera revealed by two-photon excited fluorescence microscopy (Oct). Invest Ophthalmol. Vis. Sci. 57 (13), 5602–5610. https://doi.org/10.1167/IOVS.16-19706.

Piano, I., et al., 2020. Myriocin effect on tvrm4 retina, an autosomal dominant pattern of retinitis pigmentosa (May). Front Neurosci. 14, 488223. https://doi.org/10.3389/FNINS.2020.00372/BIBTEX.

Piano, I., Novelli, E., Gasco, P., Ghidoni, R., Strettoi, E., Gargini, C., 2013. Cone survival and preservation of visual acuity in an animal model of retinal degeneration (Jun). Eur. J. Neurosci. 37 (11), 1853–1862. https://doi.org/10.1111/EJN.12196.

Platania, C.B.M., et al., 2019b. Novel ophthalmic formulation of myriocin: implications in retinitis pigmentosa (Jan). Drug Deliv. 26 (1), 237–243. https://doi.org/10.1080/10717544.2019.1574936.

Platania, C.B.M., et al., 2019a. Novel ophthalmic formulation of myriocin: implications in retinitis pigmentosa (Jan). Drug Deliv. 26 (1), 237–243. https://doi.org/10.1080/10717544.2019.1574936.

Quigley, H.A., 1996. Number of people with glaucoma worldwide. Br. J. Ophthalmol. 80 (5), 389–393. https://doi.org/10.1136/BJO.80.5.389.

Roberts, A.B., Russo, A., Felici, A., Flanders, K.C., 2003. Smad3: a key player in pathogenetic mechanisms dependent on TGF-β (May). Ann. N. Y Acad. Sci. 995 (1), 1–10. https://doi.org/10.1111/J.1749-6632.2003.TB03205.X.

Saika, S., et al., 2008. Fibrotic disorders in the eye: targets of gene therapy (Mar). Prog. Retin Eye Res. 27 (2), 177–196. https://doi.org/10.1016/J.PRETEYERES.2007.12.002.

Schlunck, G., Meyer-ter-Vehn, T., Klink, T., Grehn, F., 2016. Conjunctival fibrosis following filtering glaucoma surgery. Exp. Eye Res. 142, 76–82. https://doi.org/10.1016/J.EXER.2015.03.021.

Sen, E., et al., 2010. Effect of doxycycline on postoperative scarring after trabeculectomy in an experimental rabbit model (Oct). J. Ocul. Pharm. Ther. 26 (5), 399–406. https://doi.org/10.1089/JOP.2010.0064.

Shao, C.G., Sinha, N.R., Mohan, R.R., Webel, A.D., 2023. Novel therapies for the prevention of fibrosis in glaucoma filtration surgery (Mar). Biomedicines 11 (3). https://doi.org/10.3390/BIOMEDICINES11030657.

Shukla, A.G., Milman, T., Fertala, J., Steplewski, A., Fertala, A., 2023. Scar formation in the presence of mitomycin C and the anti-fibrotic antibody in a rabbit model of glaucoma microsurgery: a pilot study (Apr). Heliyon 9 (4). https://doi.org/10.1016/J.HELIYON.2023.E15368.

Signorelli, P., et al., 2021. Myriocin modulates the altered lipid metabolism and storage in cystic fibrosis (May). Cell Signal 81. https://doi.org/10.1016/J.CELLSIG.2021.109928.

Slabaugh, M., Salim, S., 2017. Use of Anti-VEGF agents in glaucoma surgery (Jan). J. Ophthalmol. 2017 (1), 1645269. https://doi.org/10.1155/2017/1645269.

Stahnke, T., et al., 2020. Suppression of the TGF-β pathway by a macrolide antibiotic decreases fibrotic responses by ocular fibroblasts in vitro (Sep). R. Soc. Open Sci. 7 (9). https://doi.org/10.1098/RSOS.200441.

Strettoi, E., et al., 2010. Inhibition of ceramide biosynthesis preserves photoreceptor structure and function in a mouse model of retinitis pigmentosa (Oct). Proc. Natl. Acad. Sci. USA 107 (43), 18706–18711. https://doi.org/10.1073/PNAS.1007644107.

Suarez-Arnedo, A., Figueroa, F.T., Clavijo, C., Arbeláez, P., Cruz, J.C., Muñoz-Camargo, C., 2020. An image J plugin for the high throughput image analysis of in vitro scratch wound healing assays (Jul). PLoS One 15 (7), e0232565. https://doi.org/10.1371/JOURNAL.PONE.0232565.

Ussher, J.R., et al., 2010. Inhibition of de novo ceramide synthesis reverses diet-induced insulin resistance and enhances whole-body oxygen consumption (Oct). Diabetes 59 (10), 2453–2464. https://doi.org/10.2337/DB09-1293.

Wilkins, M., Indar, A., Wormald, R., 2005. Intra-operative mitomycin C for glaucoma surgery (Oct.). Cochrane Database Syst. Rev. 2005 (4). https://doi.org/10.1002/14651858.CD002897.PUB2.

Wolters, J.E.J., et al., 2021. History, presence, and future of mitomycin C in glaucoma filtration surgery (Mar). Curr. Opin. Ophthalmol. 32 (2), 148–159. https://doi.org/10.1097/ICU.0000000000000729.

Wu, N., et al., 2020. Trehalose attenuates TGF-β1-induced fibrosis of hSCFs by activating autophagy (Jul). Mol. Cell Biochem 470 (1–2), 175–188. https://doi.org/10.1007/S11010-020-03760-4/FIGURES/6.

Wynn, T.A., 2008. Cellular and molecular mechanisms of fibrosis (Jan). J. Pathol. 214 (2), 199–210. https://doi.org/10.1002/PATH.2277.

Yamanaka, O., Ikeda, K., Saika, S., Miyazaki, K., Ooshima, A., Ohnishi, Y., 2006. Gene transfer of Smad7 modulates injury-induced conjunctival wound healing in mice (Aug). Mol. Vis. 12, 841–851 (Aug).

Yu, S., Tam, A.L.C., Campbell, R., Renwick, N., 2022. Emerging evidence of noncoding RNAs in bleb scarring after glaucoma filtration surgery (Apr). Cells 11 (8). https://doi.org/10.3390/CELLS11081301.

Zhang, F., et al., 2019. Rosiglitazone treatment prevents postoperative fibrosis in a rabbit model of glaucoma filtration surgery (Jun). Invest Ophthalmol. Vis. Sci. 60 (7), 2743–2752. https://doi.org/10.1167/IOVS.18-26526.

Zhang, L., Li, W., Liu, X., Guo, J., Wu, X., Wang, J., 2023. Niclosamide inhibits TGF-β1-induced fibrosis of human Tenon's fibroblasts by regulating the MAPK-ERK1/2 pathway (Oct). Exp. Eye Res 235. https://doi.org/10.1016/J.EXER.2023.109628.

Zulueta, A., et al., 2019. Inflammatory role of extracellular sphingolipids in Cystic Fibrosis (Nov). Int J. Biochem Cell Biol. 116, 105622. https://doi.org/10.1016/J.BIOCEL.2019.105622.